PERGAMON

Computers and Structures 69 (1998) 329–338

Computers & Structures

Investigation of stresses at the fixed end of deep cantilever beams

S.R. Ahmed, M.R. Khan, K.M.S. Islam, Md.W. Uddin *

Department of Mechanical Engineering, Bangladesh University of Engineering and Technology, Dhaka-1000, Bangladesh

Received 22 January 1997; accepted 28 April 1998

Abstract

A numerical investigation for the stresses and displacements of a two-dimensional elastic problem with mixed boundary conditions is reported in this paper. Specifically, it is on the analysis of stresses at the fixed end of deep cantilever beams, subjected to uniformly distributed shear at the free end. An ideal mathematical model, based on a displacement potential function, has been used to formulate the problem. The solutions are presented in the form of graphs. Results are compared with the elementary solutions and the discrepancy appears to be quite noticeable, specifically at the fixed end. The present solution shows that the fixed end of a short cantilever beam is an extremely critical zone and the elementary theory of beams completely fails to predict stresses in this zone. © 1998 Published by Elsevier Science Ltd. All rights reserved.

1. Notation

x, y	rectangular coordinates
E	elastic modulus of the material
v	Poisson's ratio
σ	stress
u	displacement component in the x-direction
v	displacement component in the y-direction
σ_x	normal stress component in the x-direction
σ_y	bending stress
σ_{xy}	shearing stress
a	beam length
b	beam depth
h	mesh length in the x-direction
k	mesh length in the y-direction
R	ratio of the mesh lengths k/h
m	number of mesh points in x-direction
n	number of mesh points in y-direction
ϕ	Airy's stress function
ψ	displacement potential function.

* Corresponding author.

2. Introduction

The elementary theories of strength of materials are unable to predict the stresses in the critical zones of engineering structures. They are very inadequate to give information regarding local stresses near the loads and near the supports of the beam. They are only approximately correct in some cases but most of the time, violate conditions which are brought to light by the more refined investigation of the theory of elasticity.

Among the existing mathematical models for two dimensional boundary-value stress problems, the two displacement function approach [1] and the stress function approach [9] are noticeable. The solution of practical problems started mainly after the introduction of Airy's stress function [9]. But the difficulties involved in trying to solve practical problems using the stress function are pointed out by Uddin [1] and also by Durelli [2]. The shortcoming of ϕ-formulation [9] is that it accepts boundary conditions in terms of loading only. Boundary restraints specified in terms of u and v can not be satisfactorily imposed on the stress function ϕ. As most of the problems of elasticity are of mixed boundary conditions, this approach fails to provide any explicit understanding of the stress distribution in

0045-7949/98/$ - see front matter © 1998 Published by Elsevier Science Ltd. All rights reserved.
PII: S0045-7949(98)00127-8

the region of restrained boundaries which are, in general, the most critical zones in terms of stress. Again, the two displacement function approach that is the u, v-formulation involves finding two functions simultaneously from two second order elliptic partial differential equations [1]. But the simultaneous evaluation of two functions, satisfying two simultaneous differential equations, is extremely difficult and this problem becomes more serious when the boundary conditions are specified as a mixture of restraints and stresses. As a result, serious attempts had hardly been made in the stress analysis of elastic bodies using this formulation as far as present literature is concerned.

Although elasticity problems were formulated long before, exact solutions of practical problems are hardly available because of the inability of managing the boundary conditions imposed on them. The age-old S-Venant's principle is still applied and its merit is evaluated in solving problems of solid mechanics [3, 4] in which full boundary effects could not be taken into account satisfactorily. Actually, management of boundary conditions and boundary shapes are the main obstacles to the solution of practical problems. The reason for the birth and dominance of the finite element method is merely its superiority in managing the boundary conditions. In circumventing this problem, Dow, Jones and Harwood [5] have introduced a new boundary modeling approach for finite-difference applications of displacement formulation of solid mechanics and solved the problem of a uniformly loaded cantilever beam. In this connection, they reported that the accuracy of the finite difference method in reproducing the state of stresses along the boundary was much higher than that of finite element analysis. However, they have noted that the computational effort of the finite difference analysis, under the new boundary modeling, is even somewhat greater than that of finite element analysis. Even now, photoelastic studies are being carried out for classical problems like uniformly loaded beams on two supports [2, 6], only because boundary effects could not be fully taken into account in their analytical method of solutions.

As stated above, neither of the formulations is suitable for solving problems of mixed boundary conditions and hence an ideal mathematical model is used here. In this numerical approach, the problem has been formulated in terms of a single potential function, ψ [1, 10], defined in terms of displacement components, and is considered as parallel to the stress function ϕ since both of them have to satisfy the same bi-harmonic equation.

3. Formulation of the problem

Fortunately, almost all the practical problems of stress analysis can easily be resolved into two-dimensional problems. A large number of these practical problems of elasticity are covered by one of the two simplifying assumptions, namely, either of plane stress or of plane strain. With reference to a rectangular coordinate system, the three governing equations in terms of the stress variables σ_x, σ_y, and σ_{xy} for plane stress and plane strain problems are given by

$$\frac{\partial \sigma_x}{\partial x} + \frac{\partial \sigma_{xy}}{\partial y} = 0, \tag{1}$$

$$\frac{\partial \sigma_y}{\partial y} + \frac{\partial \sigma_{xy}}{\partial x} = 0, \tag{2}$$

$$\left(\frac{\partial^2}{\partial x^2} + \frac{\partial^2}{\partial y^2}\right)(\sigma_x + \sigma_y) = 0. \tag{3}$$

If we replace the stress functions in Eqs. (1)–(3) by displacement functions u (x, y) and v (x, y), which are related to stress functions through the expressions

$$\sigma_x = \frac{E}{1 - v^2}\left[\frac{\partial u}{\partial x} + v\frac{\partial v}{\partial y}\right], \tag{4}$$

$$\sigma_y = \frac{E}{1 - v^2}\left[\frac{\partial v}{\partial y} + v\frac{\partial u}{\partial x}\right], \tag{5}$$

$$\sigma_{xy} = \frac{E}{2(1 + v)}\left[\frac{\partial u}{\partial y} + \frac{\partial v}{\partial x}\right], \tag{6}$$

then Eq. (3) is redundant and Eqs. (1) and (2) transform to

$$\frac{\partial^2 u}{\partial x^2} + \left(\frac{1 - v}{2}\right)\frac{\partial^2 u}{\partial y^2} + \left(\frac{1 + v}{2}\right)\frac{\partial^2 v}{\partial x \partial y} = 0, \tag{7}$$

$$\frac{\partial^2 v}{\partial y^2} + \left(\frac{1 - v}{2}\right)\frac{\partial^2 v}{\partial x^2} + \left(\frac{1 + v}{2}\right)\frac{\partial^2 u}{\partial x \partial y} = 0 \tag{8}$$

where u and v are the displacement components of a point in the x and y-directions, respectively. The equilibrium Eqs. (7) and (8) have to be solved now for the case of a two-dimensional problem when the body forces are assumed to be absent.

In the present approach, the problem is reduced to the determination of a single variable instead of evaluating two functions, u and v, simultaneously, from equilibrium Eqs. (7) and (8). In this case, as in the case of Airy's stress function ϕ, a potential function ψ (x, y) is defined in terms of displacement components as

$$u = \frac{\partial^2 \psi}{\partial x \partial y},$$

$$v = -\frac{1}{1+\nu}\left[(1-\nu)\frac{\partial^2 \psi}{\partial y^2} + 2\frac{\partial^2 \psi}{\partial x^2}\right].$$

When the displacement components in the Eqs. (7) and (8) are replaced by their expressions in terms of $\psi(x, y)$, as defined above, Eq. (7) is automatically satisfied and the only condition that ψ has to satisfy becomes [1]

$$\frac{\partial^4 \psi}{\partial x^4} + 2\frac{\partial^4 \psi}{\partial x^2 \partial y^2} + \frac{\partial^4 \psi}{\partial y^4} = 0. \tag{9}$$

Therefore, the whole problem has been formulated in such a way that a single function ψ has to be evaluated from the bi-harmonic Eq. (9) associated with the boundary conditions that are specified at the bounding edges of the beam.

4. Boundary conditions

The practical problems in elasticity are normally of the boundary-value type where the conditions that are imposed on the boundary of the elastic body are visualized either in terms of edge-fixity or edge-loading, that is, known values of displacements and stresses at the boundary. Referring to Fig. 1, which illustrates the present problem of cantilever beam, both the top and bottom edges are free from loading, the left lateral edge is fixed and the right lateral edge is subjected to uniformly distributed shear.

For both the top and bottom edges, AB and CD, the normal and tangential stress components, stated mathematically, are given by

$$\sigma_x(x, y) = 0, \quad \text{and}$$

$$\sigma_{xy}(x, y) = 0, \quad \text{for} \quad 0 \le y/a \le 1, \; x/b = 0 \quad \text{and} \quad 1.$$

For the left lateral edge, AC, the normal and tangential displacement components are, respectively,

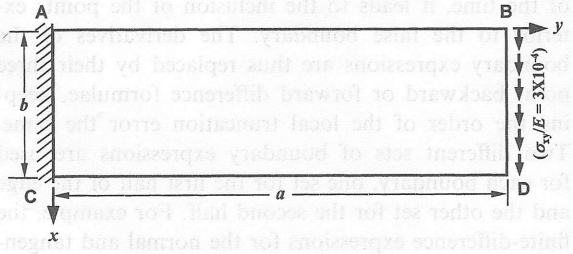

Fig. 1. Deep cantilever beam subjected to uniformly distributed shear at the free end.

$$u(x, y) = 0, \quad \text{and}$$

$$v(x, y) = 0, \quad \text{for} \quad 0 \le x/b \le 1, \; y/a = 0,$$

and the corresponding boundary conditions for the right lateral edge, BD, the normal and tangential stresses are

$$\sigma_y(x, y) = 0,$$

$$\sigma_{xy}(x, y)/E = 3.0 \times 10^{-4} \quad \text{for} \quad 0 \le x/b \le 1, \; y/a = 1.$$

In order to solve the problem using Eq. (9), the boundary conditions are also needed to be expressed in terms of ψ and thus the corresponding relations between known functions on the boundary and the function ψ are,

$$u(x, y) = \frac{\partial^2 \psi}{\partial x \partial y}, \tag{10}$$

$$v(x, y) = -\frac{1}{1+\nu}\left[(1-\nu)\frac{\partial^2 \psi}{\partial y^2} + 2\frac{\partial^2 \psi}{\partial x^2}\right], \tag{11}$$

$$\sigma_x(x, y) = \frac{E}{(1+\nu)^2}\left[\frac{\partial^3 \psi}{\partial x^2 \partial y} - \nu\frac{\partial^3 \psi}{\partial y^3}\right], \tag{12}$$

$$\sigma_y(x, y) = -\frac{E}{(1+\nu)^2}\left[\frac{\partial^3 \psi}{\partial y^3} + (2+\nu)\frac{\partial^3 \psi}{\partial x^2 \partial y}\right], \tag{13}$$

$$\sigma_{xy}(x, y) = \frac{E}{(1+\nu)^2}\left[\nu\frac{\partial^3 \psi}{\partial x \partial y^2} - \frac{\partial^3 \psi}{\partial x^3}\right]. \tag{14}$$

As far as numerical computation is concerned, it is evident from the expressions of above conditions that all the boundary conditions of interest can easily be discretized in terms of the displacement function ψ by the method of finite-difference.

5. Solution procedure

The essential feature of the numerical approach here is that the original governing differential equations of the boundary-value problems are replaced by a finite set of simultaneous algebraic equations and the solutions of this set of simultaneous algebraic equations provide us with an approximation for the displacement and stress within the solid body. About the solution through the proposed formulation, attention may be drawn to the points described below.

5.1. Method of solution

The limitation and complexity associated with analytical solutions [7] leads to the conclusion that a numerical modeling for this class of problem is the only

plausible approach. The finite-difference technique, one of the oldest numerical methods extensively used for solving differential equations, is used here to transform the fourth order bi-harmonic partial differential Eq. (9) and also the partial differential Eqs. (10)–(14), associated with the boundary conditions, into their corresponding algebraic equations. The discrete values of the potential function, ψ (x, y), at the mesh points of the domain concerned (Fig. 2) are obtained from a system of linear algebraic equations resulting from the discretization of the governing equation and the prescribed boundary conditions.

The region in which the dependent function is to be evaluated is divided into a desirable number of mesh points and the values of the function ψ are sought only at these points. To keep the order of the error of the difference equations of the boundary conditions to a minimum, a new false boundary, exterior to the physical domain, is introduced. The discretization scheme for the domain concerned is illustrated in Fig. 2. The division into mesh points can be done in any regular or irregular manner, but considering the rectangular shape of the boundary and also the nature of the differential equations involved, rectangular grid points are used all over the region concerned. The governing bi-harmonic equation which is used to evaluate the function only at the internal mesh points is expressed in its corresponding difference equation using central difference operators. When all the derivatives present in the bi-harmonic equation are replaced by their respective central difference formulae, the complete finite-difference equation for bi-harmonic Eq. (9) becomes

$$\begin{aligned} &R^4\{\psi(i-2,j)+\psi(i+2,j)\}-4R^2)(1+R^2)\{\psi(i-1,j)\\ &\quad+\psi(i+1,j)\}-4(1+R^2)\{\psi(i,j+1)+\psi(i,j-1)\}\\ &\quad+(6R^4+8R^2+6)\psi(i,j)+2R^2\{\psi(i-1,j-1)\\ &\quad+\psi(i-1,j+1)+\psi(i+1,j-1)\\ &\quad+\psi(i+1,j+1)\}+\psi(i,j-2)+\psi(i,j+2)=0 \end{aligned} \tag{15}$$

where $R = k/h$.

Considering an interior mesh point O (i, j), it is seen that the algebraic Eq. (15) contains the discretized variable of the 13 neighboring mesh points, and when O becomes an immediate neighbor of the physical boundary mesh points, this equation will contain mesh points exterior to the boundary as well as on the boundary itself (Fig. 2). Thus, the application of the central difference expression of the bi-harmonic equation to the points in the immediate neighborhood of the physical boundary will cause no difficulties, provided an imaginary false boundary exterior to the physical boundary is introduced.

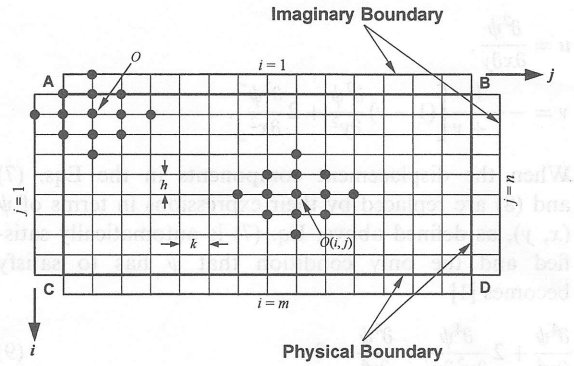

Fig. 2. Rectangular mesh-network of the domain in relation to the coordinates system and the finite-difference discretization of the bi-harmonic equation at an arbitrary internal mesh point.

5.2. Management of boundary conditions

Normally, the boundary conditions are specified either in terms of loadings or of restraints or of some combination of the two. Each mesh point on the physical boundary of the domain always entertains two boundary conditions at a time out of four possible, namely, (1) normal stress and shear stress; (2) normal stress and tangential displacement; (3) shear stress and normal displacement; and (4) normal displacement and tangential displacement. The computer program is organized here in such a fashion that, out of these two conditions, one is used for evaluation of ψ at the concerned boundary point and the other one for the corresponding point on the exterior false boundary. Thus, when the boundary conditions are expressed by their appropriate difference equations, every mesh point of the domain will have a single linear algebraic equation. Table 1 lists the boundary conditions for each boundary of the beam along with the corresponding choice of mesh points on the boundary.

As the differential equations associated with the boundary conditions contain second and third order derivatives of the function ψ, the application of the central difference expression is not practical as, most of the time, it leads to the inclusion of the points exterior to the false boundary. The derivatives of the boundary expressions are thus replaced by their three point backward or forward difference formulae, keeping the order of the local truncation error the same. Two different sets of boundary expressions are used for each boundary, one set for the first half of the edge and the other set for the second half. For example, the finite-difference expressions for the normal and tangential components of stress on the top boundary, AB, at points closer to A, are given by:

Table 1
Specification of the boundary conditions in relation to corresponding mesh-points on the boundary

Boundary	Given boundary conditions	Correspondence between mesh-points and given boundary conditions	
		Condition/mesh-point	Condition/mesh-point
Top, AB	σ_x, σ_{xy}	$\sigma_x/(2,j)$	$\sigma_{xy}/(1,j)$
Bottom, CD	σ_x, σ_{xy}	$\sigma_x/(m-1,j)$	$\sigma_{xy}/(m,j)$
Left, AC	u, v	$u/(i,2)$	$v/(i,1)$
Right, BD	σ_y, σ_{xy}	$\sigma_{xy}/(i,n-1)$	$\sigma_y/(i,n)$

$$\sigma_x(2,j) = \frac{Ev}{(1+v)^2R^3h^3}\left[\left(\frac{3R^2}{v}-5\right)\psi(2,j) + 1.5\psi(2,j-1) + \left(6-\frac{4R^2}{v}\right)\psi(2,j+1) + \left(\frac{R^2}{v}-3\right)\psi(2,j+2) + 0.5\psi(2,j+3) - \frac{3R^2}{2v}\{\psi(1,j)+\psi(3,j)\} + \frac{2R^2}{v}\{\psi(1,j+1)+\psi(3,j+1)\} - \frac{R^2}{2v}\{\psi(1,j+2)+\psi(3,j+2)\}\right], \quad (16)$$

$$\sigma_{xy}(2,j) = \frac{Ev}{(1+v)^2R^2h^3}\left[\frac{3R^2}{2v}\psi(1,j) + \left(3-\frac{5R^2}{v}\right)\psi(2,j) + \left(\frac{6R^2}{v}-4\right)\psi(3,j) + \left(1-\frac{3R^2}{v}\right)\psi(4,j) + \frac{R^2}{2v}\psi(5,j) - 1.5\{\psi(2,j-1)+\psi(2,j+1)\} + 2\{\psi(3,j-1)+\psi(3,j+1)\} - 0.5\{\psi(4,j-1) + \psi(4,j+1)\}\right]. \quad (17)$$

The discretization scheme using the neighboring grid-points as required for expressing the above conditions on the top boundary of the beam, AB, is illustrated in Fig. 3. Special treatments are also adopted for the corner mesh points which are generally points of 'transition' in the boundary conditions. Referring to Fig. 4, assuming B as the corner mesh point, it is seen that B is a common point of both the edges AB and BD and thus it has four boundary conditions—two from each edge. In solving the present beam problem, three conditions out of the four are used, the remaining one is treated as redundant. The three conditions mentioned above are organized in such a way that the values of ψ at three points, namely, 1, B, and 2 are evaluated from these equations—points 1 and B from the boundary conditions coming from edge AB and point 2 from the boundary equation from edge BD. Table 2 shows the choices and the conditions to be satisfied by the corner mesh points in relation to the present cantilever beam problem. An example of the finite-difference discretization used to evaluate the corner mesh point 2 is shown in Fig. 4 and the corresponding difference equation is as follows:

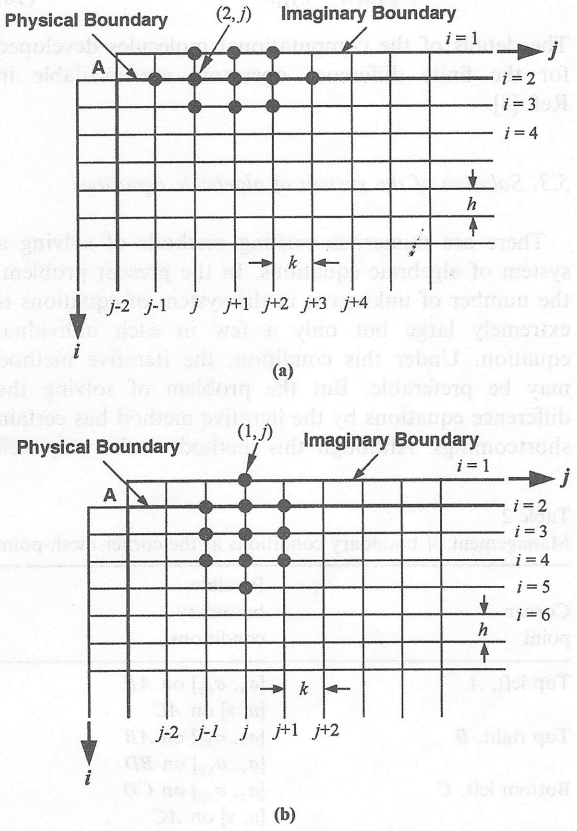

Fig. 3. Grid-points for expressing the boundary conditions on the top edge at points closer to A, (a) for normal stress component, σ_x (b) for tangential stress component, σ_{xy}.

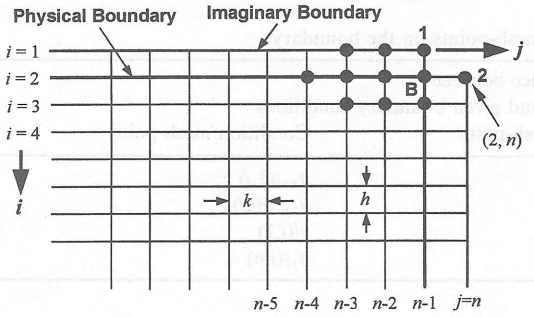

Fig. 4. Grid-points used in expressing the boundary condition σ_y for mesh point 2.

$$\sigma_y(2,n-1)=\frac{-E}{(1+v)^2R^3h^3}[1.5\psi(2,n)-\{5+3R^2(2+v)\}\times\psi(2,n-1)+\{6+4R^2(2+v)\}\psi(2,n-2)-\{3+R^2(2+v)\}\psi(2,n-3)+0.5\psi(2,n-4)+1.5R^2(2+v)\{\psi(1,n-1)+\psi(3,n-1)\}-2R^2(2+v)\{(\psi 1,n-2)+\psi(3,n-2)\}+0.5R^2(2+v)\{\psi(1,n-3)+\psi(3,n-3)\}]. \quad (18)$$

The details of the computational molecules developed for the finite difference operators are available in Ref. [8].

5.3. Solution of the system of algebraic equations

There are numerous existing methods of solving a system of algebraic equations. In the present problem, the number of unknowns in the system of equations is extremely large but only a few in each individual equation. Under this condition, the iterative method may be preferable. But the problem of solving the difference equations by the iterative method has certain shortcomings. Although this method works very well for certain boundary conditions, it fails to produce any solution for other complex boundary conditions. In certain cases, the rate of convergence of iteration is extremely slow, which makes it impractical. As this iterative method has the limitation of not always converging to a solution and sometimes converging but very slowly, the authors have thus used a triangular decomposition method ensuring better reliability and better accuracy of solution in a shorter period of time. The matrix decomposition method, used here, solves the present system of equations directly. Finally, the same difference equations as those of the boundary conditions are organized for the evaluation of displacement and stress components at different sections of the beam from the known values of ψ.

6. Results and discussion

Numerical solution with mixed and variable boundary conditions has rarely been attempted as the boundary conditions of these practical elastic problems pose serious difficulty in their solutions. This problem has been satisfactorily tackled by present formulation. All the solutions of interest obtained through the ψ-formulation conform to the symmetric and anti-symmetric characteristics of the problem and also to the famous S-Venant's principle that the effects of sharp variation of a parameter on the boundary die down and become uniform with the increase of distance of points in the body from the boundary.

In obtaining numerical values for the present problem, the beam as the elastic body is assumed to be made of ordinary steel ($v = 0.3$, $E = 200$ GPa). Graphs are plotted at different constant values of x for varying y as well as at constant y for varying x for the parameters of interest. Moreover, the effect of a/b ratio on the relevant displacement and stress components is explicitly illustrated here. In order to make the results non-dimensional, the displacements are

Table 2
Management of boundary conditions at the corner mesh-points

Corner point	Possible boundary conditions	Conditions used	Corresponding mesh-points for evaluation of ψ
Top left, A	$[\sigma_x, \sigma_{xy}]$ on AB $[u, v]$ on AC	$[\sigma_x,\sigma_{xy},v]$	(2,2), (1,2), (2,1)
Top right, B	$[\sigma_x, \sigma_{xy}]$ on AB $[\sigma_y, \sigma_{xy}]$ on BD	$[\sigma_x,\sigma_{xy},\sigma_y]$	(2,$n-1$), (1,$n-1$), (2,n)
Bottom left, C	$[\sigma_x, \sigma_{xy}]$ on CD $[u, v]$ on AC	$[\sigma_x,\sigma_{xy},v]$	($m-1$,2), (m,2), ($m-1$,1)
Bottom right, D	$[\sigma_x,\sigma_{xy}]$ on CD $[\sigma_y, \sigma_{xy}]$ on BD	$[\sigma_x,\sigma_{xy},\sigma_y]$	($m-1$,$n-1$), (m,$n-1$), ($m-1$,n)

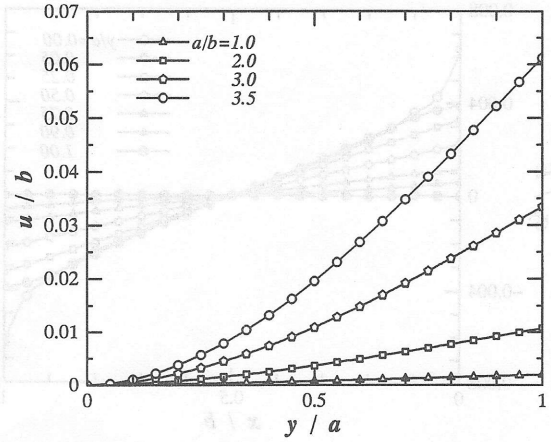

Fig. 5. Distribution of the displacement component u along the neutral axis of deep cantilever beams.

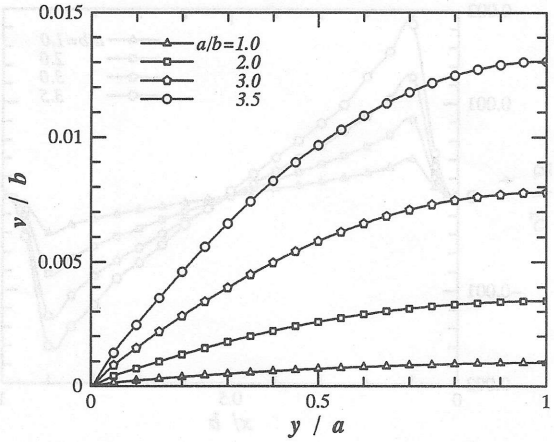

Fig. 7. Distribution of the displacement component v along the top boundary ($x/b = 0$) of deep cantilever beams.

expressed as the ratio of actual displacement to the depth of the beam and the stresses as the ratio of the actual stress to the elastic modulus of the beam material.

Fig. 5 shows the distribution of displacement component u along the neutral axis of the beam. It is observed to be nonlinear in nature and identical with the elementary solution having third order polynomial-like behavior. The general trend of the curve reveals that the displacement is zero at the fixed end and maximum at the free end of the cantilever beam which is in complete conformity with the loading as well as with the end conditions. The effect of the a/b ratio on the distribution of u along the neutral axis is also illustrated in the same figure. It conforms to the fact that, at a lower a/b ratio, the end-effects become very prominent and provide restriction to the deflection of the beam.

From the distribution of the displacement component v with respect to y in Fig. 6, it is seen that this displacement at the free end for a particular a/b ratio is maximum at the top and bottom fibers, but zero over the whole depth at the fixed end and all along the neutral axis, which is fully in conformity with the physical model of the problem. The distribution is completely asymmetric about the neutral axis of the beam, which conforms to the assumption of the elementary theory of beam that plane sections remain plane during the bending of beams.

The distribution of the displacement component v over the span is presented in Fig. 7 describing the effect of the a/b ratio on the distribution at the top

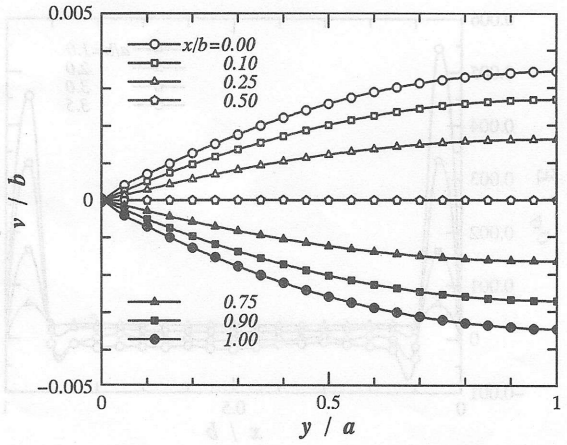

Fig. 6. Distribution of the displacement component v at various longitudinal sections of the cantilever beams ($a/b = 2$).

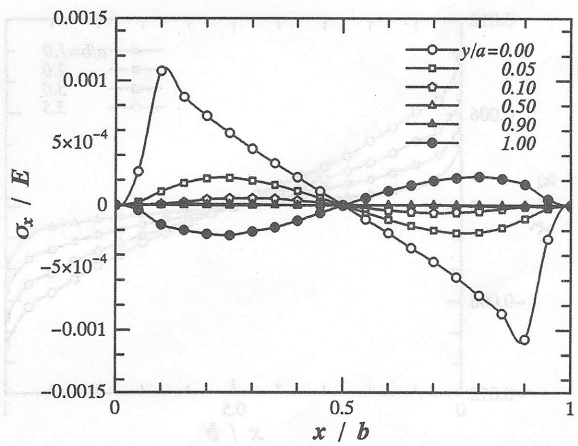

Fig. 8. Distribution of normal stress component σ_x at various transverse sections of a deep cantilever beam ($a/b = 2.5$).

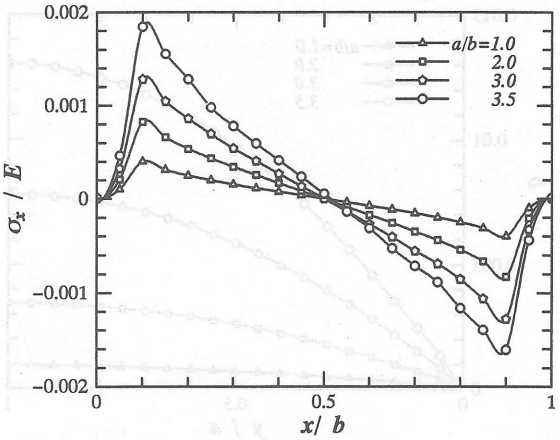

Fig. 9. Distribution of the normal stress component σ_x at the fixed end of deep cantilever beams.

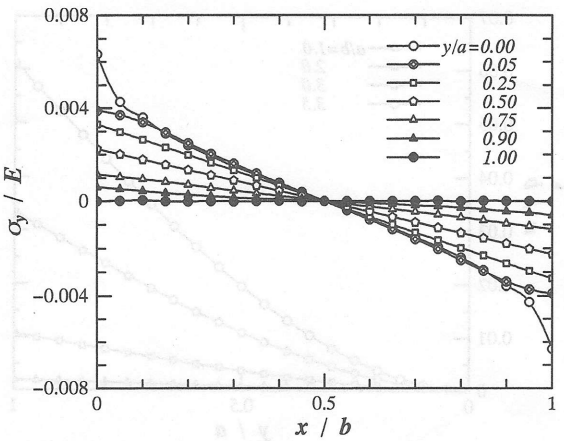

Fig. 11. Distribution of bending stress σ_y over various transverse sections of a deep cantilever beam (a/b = 2.5).

edge of the beam. Displacement in the direction of y also increases substantially towards the free end as the beam becomes longer.

Fig. 8 shows the distribution of normal stress component σ_x with respect to x at various transverse sections of the beam. From the distribution, it is observed that the variation is sinusoidal in nature and the fixed edge is the most critical section of the beam as far as the normal stress is concerned. The effect of the a/b ratio on the distribution of σ_x at the fixed end of the beam is illustrated in Fig. 9. As appears from the graph, stresses increase with an increasing a/b ratio for the same loading. It may be concluded from the distribution that the most critical point at the fixed end with respect to σ_x is around x/b = 0.1 and 0.9 in each of the beams.

Fig. 10 shows the variation of bending stress σ_y at the restrained boundary, showing the effect of the a/b ratio on the distribution. Stresses are maximum at both the top and bottom fibers with zero value at the mid-section which makes the distribution asymmetric about the longitudinal mid-section of the beam. It should be noted here that, for a higher a/b ratio, the magnitude of σ_y at the top fiber is higher than that at the bottom fiber. But, in cases of elementary solution, this magnitude is exactly the same for both the top and bottom fibers of the beam. Again, this variation of bending stress along the depth is analyzed for a particular beam (a/b = 2.5) mainly to compare how the elementary solutions match with that of exact solutions obtained through this numerical approach. In the elementary solution, the distribution of normal stress component varies linearly with depth everywhere and

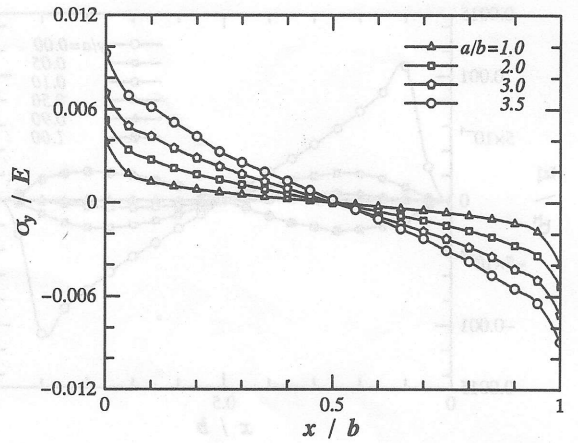

Fig. 10. Distribution of bending stress σ_y at the fixed end over the depth of deep cantilever beams.

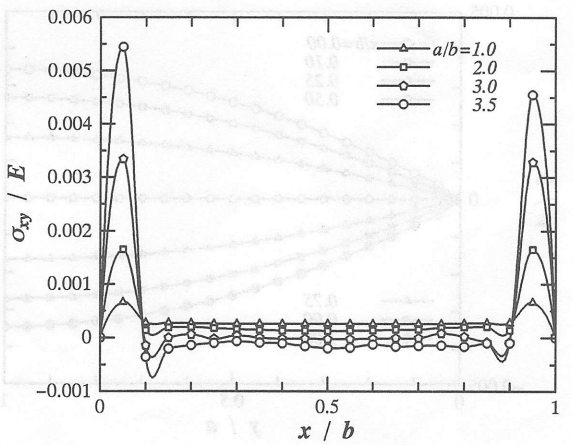

Fig. 12. Distribution of shearing stress σ_{xy} at the fixed end over the depth of deep cantilever beams.

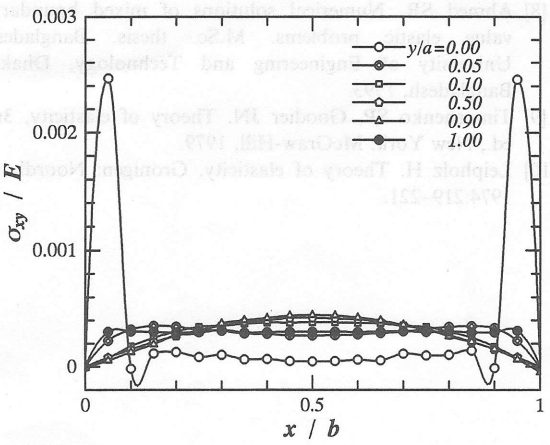

Fig. 13. Distribution of shearing stress σ_{xy} over various transverse sections of a deep cantilever beam (a/b = 2.5).

the magnitude is maximum at the top and bottom fibers. As appears from Fig. 11, the solutions differ from that of the elementary solution in a sense that the distribution is far from linear, especially, at around the fixed end, and it remains linear for other sections of the beam which, of course, conforms to the famous S-Venant's principle.

Distribution of shearing stress, σ_{xy}, at the fixed end of the cantilever beams (Fig. 12) reveals that shearing stress is zero at both the top and bottom edges which conforms to the obvious fact that both the top and bottom edges of the physical model are free from shearing stresses. The distribution describing the effect of the a/b ratio on shearing stress along the restrained boundaries, shows that the stress varies nonlinearly, having the maximum values near the top and bottom corners of the fixed edge and minimum at the mid sections which disagrees completely with the elementary solutions. Also, the beam becomes more critical in terms of shearing stresses when the length of the beam is increased, keeping the loading constant. Interestingly, for this particular type of loading, at a higher a/b ratio, the upper corner zone at the fixed end becomes more critical in terms of the stresses than the lower zone.

Finally, the variation of shearing stresses over the depth is investigated at various transverse sections of the beam mainly for comparing its characteristic behavior with the elementary solutions. From the distribution in Fig. 13, it is observed that the variation of this stress component over the depth is similar to that of elementary solutions at the mid-sections of the beam. Sufficiently away from the boundary, the distributions are parabolic in nature and they are identical in nature and magnitude with that of elementary solutions. From the elementary solution it is observed that the magnitude of the shearing stresses are maximum at the mid-section of the beam. This is not agreed upon by our numerical solutions and it differs mainly around the fixed ends as predicted by the elementary theory; it is maximum at about x/b = 0.05 and 0.95. Since, in the elementary formulas of strength of materials, the boundary conditions are satisfied in an approximate way, it fails to provide the actual distribution of stresses at the boundaries, especially, at the restrained boundaries. The present ψ-formulation is free from this type of shortcoming and is thus capable of providing the actual stress distribution at any critical section, either at or far from the restrained edges.

7. Conclusions

Earlier mathematical models of elasticity were very deficient in handling the practical problems. No appropriate approach was available in the literature which could provide the explicit information about the actual distribution of stresses at the critical regions of restrained boundaries satisfactorily. The distinguishing feature of the present ψ-formulation over the existing approaches is that, here, all modes of boundary conditions can be satisfied exactly, whether they are specified in terms of loading or physical restraints or any combination of them and thus the solutions obtained are promising and satisfactory for the entire region of interest.

Both the qualitative and quantitative results of deep cantilever beams, obtained through the ψ-formulation, establish the soundness and appropriateness of the present approach. The comparative study with elementary solutions verifies that the elementary solutions are highly approximate as they fail to provide the solutions in the neighborhood of restrained boundaries.

References

[1] Uddin MW. Finite difference solution of two-dimensional elastic problems with mixed boundary conditions. M.Sc. thesis. Carleton University, Canada, 1966.
[2] Durelli AJ, Ranganayakamma B. Parametric solution of stresses in beams. J Engng Mech 1989;115(2):401.
[3] Horgan CO, Knowels JK. Recent development concerning S-Venant's principle. Adv Appl Mech 1983;23:179–269.
[4] Parker DF. The role of S-Venant's solutions in rod and beam theories. J Appl Mech 1979;46:861–6.
[5] Dow JO, Jones MS, Harwood SA. A new approach to boundary modeling for finite difference applications in solid mechanics. Int J Numer Meth Engng 1990;30:99–113.

[6] Durelli AJ, Ranganayakamma B. On the use of photoelasticity and some numerical methods. Photomech Speck Metrol, SPIE 1987;814:1–8.

[7] Idris ABM. A new approach to solution of mixed boundary-value elastic problems. M.Sc. thesis. Bangladesh University of Engineering and Technology, Dhaka, Bangladesh, 1993.

[8] Ahmed SR. Numerical solutions of mixed boundary-value elastic problems. M.Sc. thesis. Bangladesh University of Engineering and Technology, Dhaka, Bangladesh, 1993.

[9] Timoshenko SP, Goodier JN. Theory of elasticity, 3rd ed., New York: McGraw-Hill, 1979.

[10] Leipholz H. Theory of elasticity. Gronigen: Noordhoff, 1974:219–221.